

Photovoltaic Properties of Cu_2S -CdS Heterojunctions*

W. D. GILL† AND R. H. BUBE

Department of Materials Science, Stanford University, Stanford, California 94305

(Received 26 March 1970)

The photovoltaic properties of Cu_2S -CdS heterojunctions have been compared before and after short heat treatment, using measured I - V characteristics, junction capacitance, and spectral response. After heat treatment slow transients in the photoresponse and effects of secondary illumination were investigated. Optical quenching of the photocurrent was observed in two ir bands corresponding to transitions at 0.8 and 1.1 eV, and enhancement of the photocurrent was seen for $h\nu > 1.5$ eV. Long persistence of the enhancement effect was observed, which thermally quenched with an activation energy of 0.95 eV. A model for the heterojunction is proposed in which hole trapping in deep imperfection centers in the CdS near the junction is the key mechanism. A conduction band spike is assumed to exist at the Cu_2S -CdS interface. The transparency of this spike to photoexcited electrons diffusing from the Cu_2S is modulated by variations in the CdS depletion width caused by the deep trapping.

INTRODUCTION

The Cu_2S -CdS heterojunction has received considerable attention as an efficient photovoltaic cell for solar-energy conversion.¹⁻⁶ Short heat treatment of the heterojunctions has been a usual step in obtaining the highest efficiency cells. After heat treatment several unusual features are seen in the cell characteristics. These features include the crossover of the forward light and dark I - V characteristics, slow transient components in the photoresponse, and changes in the cell spectral response under various secondary light conditions.⁶⁻⁹ Work on high-efficiency Cu_2S -CdS heterojunctions has established that the major part of the photoresponse is due to light absorption in the Cu_2S followed by electron diffusion to the Cu_2S -CdS interface.^{5,6} The I - V characteristics, slow transients, and effect of secondary light on the spectral response were attributed to photoconductivity of a p -type insulating CdS layer at the interface affecting the series resistance and effective-barrier height of the heterojunction.

Measurements of the ambipolar diffusion lengths in Cu_2S and CdS have been made on nonheat-treated heterojunctions and were reported in a previous paper.¹⁰ In this paper we propose a new model for the Cu_2S -CdS heterojunction based on a wide range of experiments made on cells before and after heat treatment. In the proposed mechanism electrons diffusing across the junction from the Cu_2S must tunnel through a conduction band spike at the interface. In postheat-treatment cells, the tunneling probability is controlled by the occupancy of deep-lying imperfection levels in the CdS depletion region.

EXPERIMENTAL

Sample Preparation

Single crystals of undoped nonstoichiometric ≈ 1 (Ωcm)⁻¹ CdS were cut to form $2 \times 5 \times 0.5$ -mm samples with the c axis perpendicular to the platelets. The source of the CdS crystals was Clevite Corporation with the exception of one crystal grown at Stanford. The large

faces of the platelets were polished using $0.3\text{-}\mu$ alumina. Ohmic contacts were made to one of the large surfaces by vapor deposition of indium followed by short heating. The other polished surface was masked, and then etched in a solution of potassium permanganate in concentrated H_2SO_4 for 2 min.

The masked crystals were then immersed in a hot (80°C) saturated solution of CuCl in distilled water. Hydroxyl amine hydrochloride and HCl were added to the solution to ensure reduction of all the copper ions to the Cu^+ state. Dipping time varied depending on the desired Cu_2S layer thickness, CdS orientation, and surface treatment. To obtain thin (0.1 - $0.5\text{ }\mu\text{m}$) semi-transparent Cu_2S layers suitable for front-wall illumination, dipping times from 1 to 5 min were used.

Contact to the Cu_2S layer was made by attaching copper wires with silver paint either directly to the Cu_2S or onto evaporated-gold dots on the Cu_2S .

Heat Treatment

Heating of the cell was carefully avoided once the heterojunction was formed until a complete set of preheat-treatment electrical and photovoltaic measurements were obtained. Subsequently, the cells were heat treated at 250°C in air for times varying from 15 sec to several minutes.

Measurements

I - V Characteristics

A Tektronix 575 Curve Tracer was used to display the I - V characteristics. Traces were obtained with the cells in the dark and under strong illumination with tungsten light. Various Corning glass filters were inserted to determine the effects of the different wavelength radiation on the I - V characteristics.

The temperature dependences of the dark forward I - V characteristics were investigated on one of the single-crystal CdS cells and on a Clevite evaporated CdS thin-film cell. These measurements were made with the sample *in vacuo*. The current and voltage were

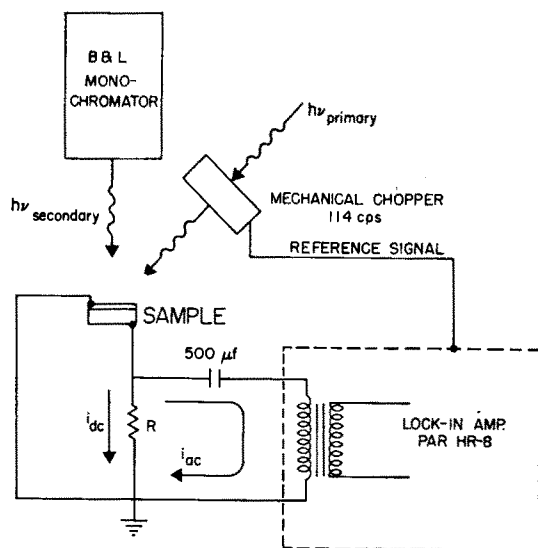


FIG. 1. Schematic of the apparatus used to measure effects of secondary radiation on the response to a primary light.

measured across the junction as the external bias voltage was varied in steps. At each temperature dark and illuminated I - V traces were also obtained using the curve tracer.

Junction Capacitance

A Boonton 75D capacitance bridge operating at 1 MHz was used to measure the junction capacitance as a function of applied voltage. The Cu_2S -CdS heterojunctions had high conductances, necessitating careful attention to sample geometry to keep the series resistance small and the conductance within the limits of the bridge.

Spectral Response

The spectral response of the short-circuit photocurrent was measured using a millimicrovoltmeter across a small series resistor. The light source was the output of a Bausch and Lomb monochromator. The light intensity was $\sim 300 \mu\text{W}/\text{cm}^2$ over most of the spectral region investigated.

Slow transients in the spectral response were followed by monitoring the output of the millimicrovoltmeter on a recorder.

Secondary Illumination Experiments

The optical enhancement and quenching of the photocurrent by a secondary light source were measured, using the apparatus shown schematically in Fig. 1. Monochromatic primary light was chopped at 114 Hz by a rotating slotted disk. A low-input impedance lock-in amplifier system was used to monitor the chopped signal. The secondary light source was the unchopped output of the monochromator.

RESULTS

I - V Characteristics

The I - V characteristics of a good Cu_2S -CdS heterojunction before and after heat treatment are shown in Fig. 2. Before heat treatment only a slight crossover of the dark and illuminated forward characteristic is seen. With strong tungsten illumination an open-circuit voltage $V_{oc} = 0.42 \text{ V}$ was measured. The part of the

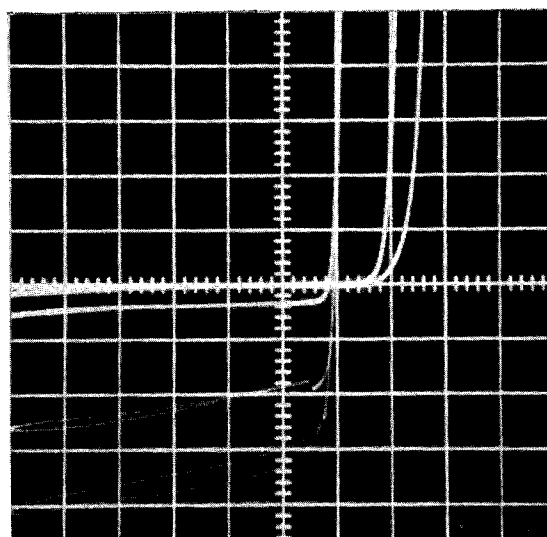
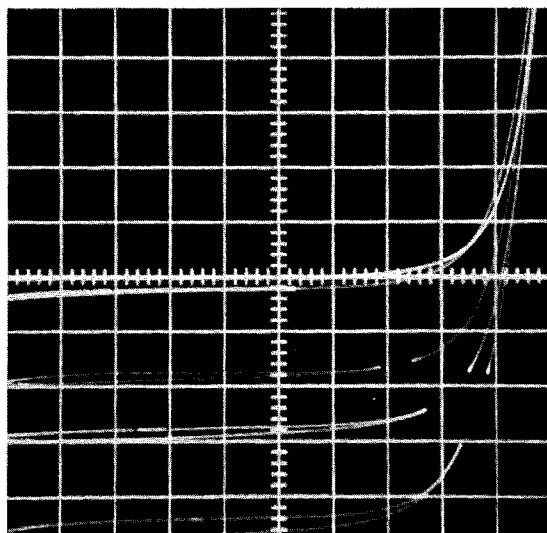


FIG. 2. I - V characteristics of a junction before and after heat treatment at 250°C for 1 min. Top: before heat treatment; vertical = $0.1 \text{ mA}/\text{div}$; horizontal = $0.1 \text{ V}/\text{div}$; illumination conditions in order of increasing I_{sc} were (1) dark, (2) $0.36 \mu\text{m} < \lambda < 0.6 \mu\text{m}$, (3) $0.3 \mu\text{m} < \lambda < 1.0 \mu\text{m}$, (4) $\lambda > 0.65 \mu\text{m}$, (5) unfiltered tungsten radiation. Bottom: after heat treatment; Vertical = $0.05 \text{ mA}/\text{div}$; horizontal = $0.5 \text{ V}/\text{div}$; illumination conditions (1) dark, (2) $\lambda > 0.65 \mu\text{m}$, (3) $0.36 \mu\text{m} < \lambda < 0.6 \mu\text{m}$, (4) $0.3 \mu\text{m} < \lambda < 1.0 \mu\text{m}$, (5) unfiltered tungsten radiation.

characteristic lying in the fourth quadrant, representing power produced by the cell, is very square, filling 84% of the area given by the product $I_{sc}V_{oc}$. Such a square characteristic indicates low series and shunt losses in the cell. Cells with similar I - V characteristics could be consistently made on carefully prepared CdS surfaces. Heat treatment was always detrimental to the photovoltaic properties of such cells.

The I - V characteristics obtained after a 1-min heat treatment are shown in the lower photograph of Fig. 2. The most noticeable change is in the forward dark current, which at 0.5 V has decreased some five orders of magnitude from the preheat-treatment value. Under illumination with light having $\lambda > 0.65 \mu\text{m}$ a partial recovery of the forward current is seen, while under tungsten illumination or illumination with light having $\lambda < 0.65 \mu\text{m}$ the forward current is almost identical to the preheat-treatment curve. From Fig. 2, the postheat-treatment V_{oc} is 0.48 V, and I_{sc} has decreased to $\frac{1}{3}$ of the preheat-treatment value. The part of the illuminated characteristic in the fourth quadrant still fills $\sim 84\%$ of the $I_{sc}V_{oc}$ product.

Many cells were prepared which had poor I - V characteristics before heat treatment. These cells generally showed improved photovoltaic properties after very

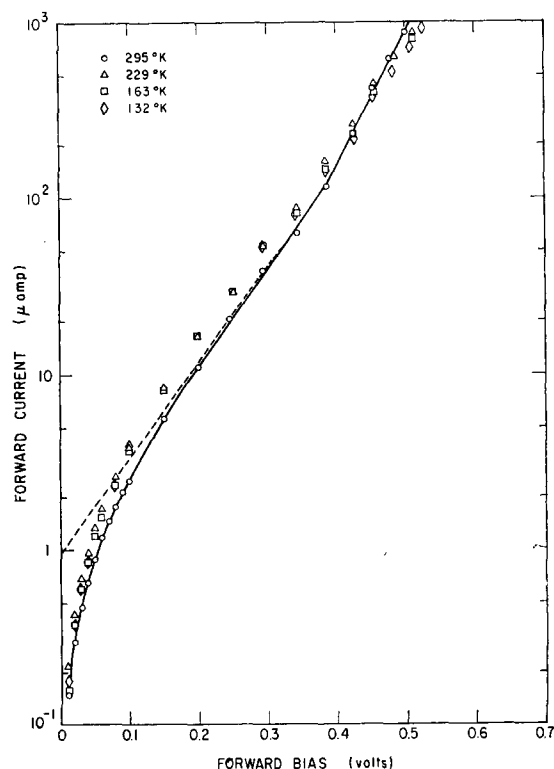


FIG. 3. Temperature dependence of forward I - V characteristics before heat treatment. The curves are drawn through data points at $T = 295^\circ\text{K}$. The dashed curve corresponds to equation $I = I_0(e^{\alpha V} - 1)$ with $\alpha = 12.5$.

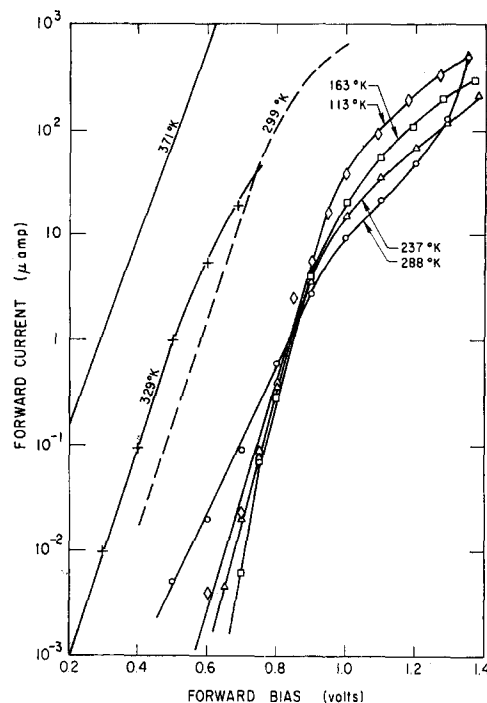


FIG. 4. Temperature dependence of forward I - V characteristics after heat treatment for 1 min at 250°C . The broken line was the stable characteristic obtained after cooling the cell from 375°K with 0.5 V applied.

short heat treatment, which could be attributed to decreased shunt losses.

The dark forward I - V characteristic of a cell before heat treatment is shown in Fig. 3 for several temperatures. At the higher currents the data has been corrected for series resistance, which varied from 8Ω at 295°K to 31Ω at 132°K . The dashed line is a fit of the equation

$$I = I_0(e^{\alpha V} - 1) \quad (1)$$

to the data at 295°K . From this data, both I_0 and α are seen to be essentially temperature independent over the range investigated. From the slope of the dashed line a value $\alpha = 12.5 \text{ V}^{-1}$ was obtained. There was almost no change in V_{oc} and I_{sc} as temperature was lowered from 295° to 135°K .

After heat treatment (1 min at 250°C) a new set of I - V characteristics was obtained at various temperatures. These curves are shown in Fig. 4. Except for the curve at 288°K the slopes of the curves were very nearly constant. Using Eq. (1) to fit the linear part of the curves, the value of α only changes from 25 V^{-1} at 113°K to 21 V^{-1} at 371°K . The curves for temperatures greater than 288°K were taken after all other measurements had been made on the cell since they represent additional heat treatment. At the higher temperatures ($T > 333^\circ\text{K}$), where $\alpha \approx \text{constant}$, the current at a fixed voltage (0.5 V) increased exponentially with an activation energy of 1.2 eV. The dashed line marked 299°K

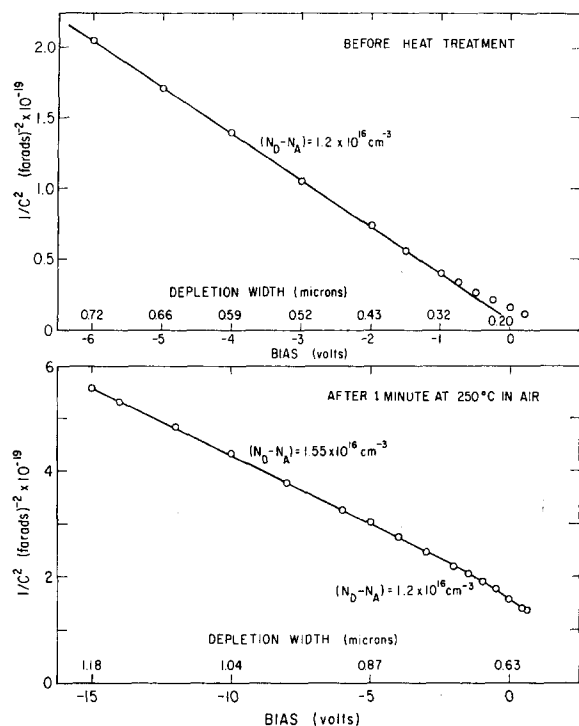


FIG. 5. $1/C^2$ versus bias voltage before and after heat treatment.

was the final characteristic and was obtained after cooling the sample from 371°K with 0.5-V forward bias applied to the cell. The large difference from the original room-temperature characteristic suggests that irreversible changes in the junction have resulted from heating to 371°K.

After heat treatment cooling the junction caused V_{oc} to increase from 0.48 V at 288°K to 0.6 V at 113°K. Small decreases in the short-circuit current were also noted.

Junction Capacitance

Capacitance-voltage characteristics before and after heat treatment are shown in Fig. 5. Linear $1/C^2$ -vs- V plots were generally obtained before heat treatment, with the slope giving values of the net donor density in good agreement with values obtained from resistivity measurements on the bulk CdS crystal. For most samples, the $1/C^2$ -vs- V plots deviated from linearity near zero bias. However, on one cell with excellent photovoltaic properties a linear plot extending into the forward bias region was obtained. The intersection with the voltage axis resulted in a diffusion potential of 1.1 V for this junction.

Short heat treatment of the cells resulted in decreased junction capacitance, indicating the formation of a narrow region of highly compensated CdS at the Cu_2S -CdS interface. In most cases the width of the compensated CdS layer was estimated from the decreased capacitance to be about 0.5- μm thick.

Strong illumination had little effect on the junction capacitance of nonheat-treated cells. After heat treatment, illumination during measurement resulted in the junction capacitance increasing several fold. After such illumination return to the dark capacitance was very slow. Rapid return to equilibrium could be accomplished by illuminating the junction with infrared light ($\lambda > 0.8 \mu\text{m}$).

Spectral Response

Before heat treatment the spectral response of the heterojunctions extends to about 1.0- μ at long wavelengths. The normalized response is shown in Fig. 6 for a junction before and after heat treatment for 1 min at 250°C. After the heat treatment, the long-wavelength edge was at 0.7 μ , and I_{sc} had decreased over the entire spectral region. The third curve in Fig. 6 shows the effect of a short-wavelength secondary light on the spectral response to the primary light. Simultaneous illumination with short-wavelength light restored the long-wavelength response of the junction while having no effect at short wavelengths.

While making spectral-response measurements, slow transients in I_{sc} were monitored. Before heat treatment the response was observed to be fast at all wavelengths. After heat treatment an initial fast response was measured followed by slow increases or decreases in I_{sc} , depending on wavelength. These initial and steady-state responses are shown in Fig. 7 for a junction after a short heat treatment. For wavelengths greater than 0.83 μm

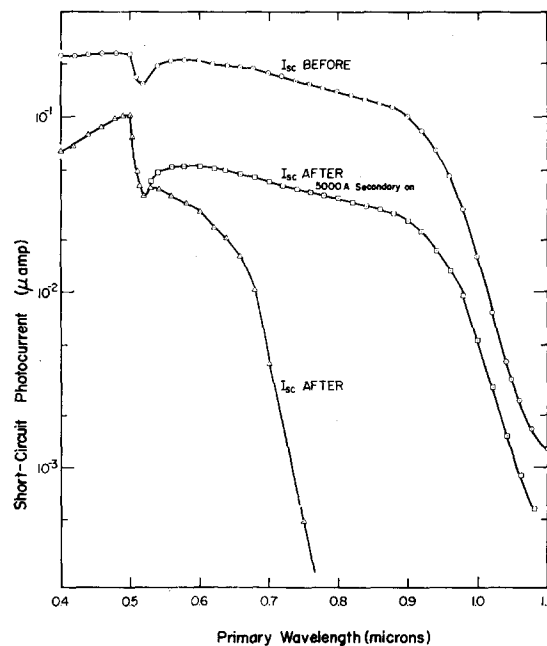


FIG. 6. Spectral response of the short-circuit photocurrent before and after heat treatment for 1 min at 250°C. The intensities of both primary and secondary light sources were 300 $\mu\text{W}/\text{cm}^2$.

I_{sc} decreased from its initial value while at shorter wavelengths I_{sc} increased.

Optical Quenching and Enhancement

The effect of secondary radiation on the primary response was measured for several primary wavelengths. The optical enhancement and quenching data shown in Fig. 8 were typical of results obtained for primary wavelengths between 0.51 and 0.83 μm . Strong quenching of the primary photocurrent was observed in two

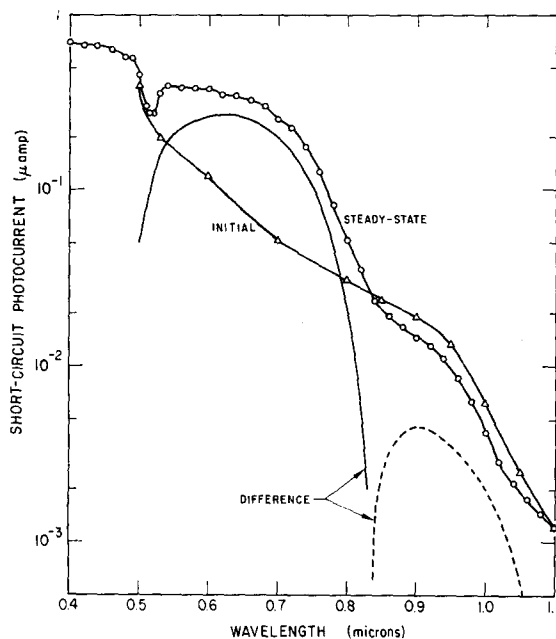


FIG. 7. Spectral response of the initial and steady-state photocurrent for a heat-treated cell. The difference curves represent the slow component of response; solid curve, enhancement; and dashed curve, quenching. Light intensity was 300 $\mu\text{W}/\text{cm}^2$.

infrared bands corresponding to transitions at 0.8 and 1.1 eV. Photocurrent enhancement was observed with short-wavelength secondary radiation. The onset of primary signal enhancement could not be evaluated easily from this data because of competition between the quenching and enhancement processes. However, changing the primary radiation to a wavelength between 0.83 and 1.0 μm resulted in only slight quenching by long-wavelength secondary light, while enhancement remained large. The onset of enhancement was then determined to be between 0.8 and 0.82 μm . This result is in good agreement with the wavelength at which the slow transient behavior changed from decreasing to increasing the initial photocurrent (Fig. 7).

Persistence of Enhanced Long-Wavelength Response

When making spectral response measurements, it was found that after illumination with wavelengths shorter than about 0.8 μm , long dark intervals were required to

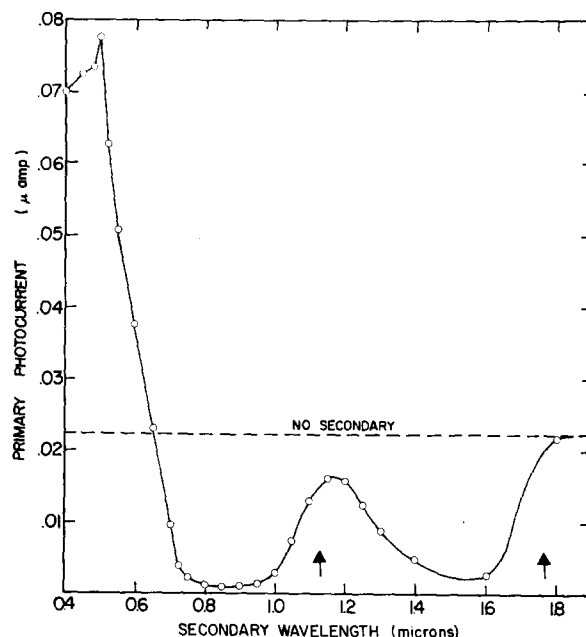


FIG. 8. Enhancement and quenching of photocurrent by secondary light. Arrows indicate where the onset of optical quenching of photoconductivity occurs in sensitive CdS crystals. Both the 0.655- μm primary and the secondary intensity were 300 $\mu\text{W}/\text{cm}^2$.

reproduce long-wavelength results. Persistence of the enhancement was measured by illuminating the junction with short-wavelength radiation for a short interval, then after a delay period with the junction in the dark, the initial response to long-wavelength illumination was recorded. Figure 9 shows the initial response as a function of the delay interval for a sample at room

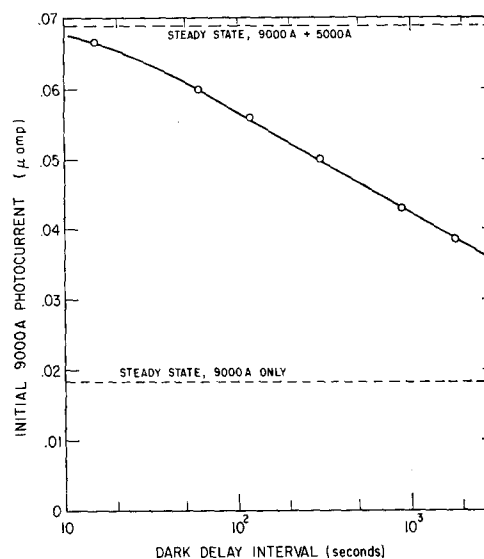


FIG. 9. Persistence of the enhancement caused by secondary light. The initial photoresponse to 0.9- μm light is plotted as a function of dark delay after switching off 0.5- μm radiation.

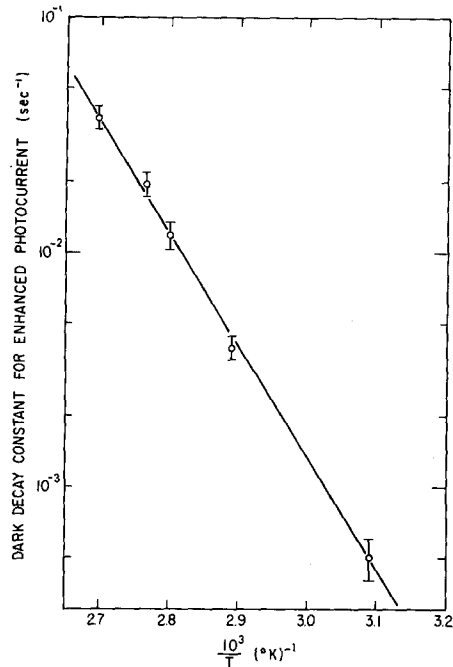


FIG. 10. Temperature dependence of the dark-decay constant for the enhanced 0.8- μ m photoresponse.

temperature. The steady-state long-wavelength response of the junction with and without short-wavelength secondary illumination is also shown in the figure.

The temperature dependence of persistence was measured by plotting the initial dark-decay rate against reciprocal temperature. Results of such a measurement are shown in Fig. 10. The slope of this plot indicates a thermal quenching process with an activation energy of 0.95 eV.

Assuming that the thermal quenching is due to emptying of trapped holes from a deep (0.95 eV) level, the data of Fig. 10 can be used to estimate the capture cross section of the level for free holes. The rate constant τ^{-1} for thermal emptying of the level is

$$\tau^{-1} = N_v S_p \nu \exp(-E/kT), \quad (2)$$

where N_v is the valence-band effective density of states, S_p is the capture cross section for free holes, ν is the thermal velocity of a hole in the valence band, and E is the energy of the level above the valence-band edge. Assuming the dark-decay constant of Fig. 10 is equal to the rate constant of Eq. (2), S_p can be determined from the intercept at $T = \infty$, which has the value $N_v S_p \nu = 2.5 \times 10^{11} \text{ sec}^{-1}$. Putting $N_v = 10^{19} \text{ cm}^{-3}$ and $\nu = 10^7 \text{ cm/sec}$ results in a value $S_p = 2.5 \times 10^{-15} \text{ cm}^2$ for the hole capture cross section.

MODEL FOR THE Cu_2S -CdS HETEROJUNCTION

The major experimental observations which must be explained by any satisfactory model of the Cu_2S -CdS

heterojunctions are (1) efficient long-wavelength response, (2) loss of long-wavelength response after heat treatment, (3) recovery or enhancement of long-wavelength response by secondary illumination, (4) slow transients in photoresponse, (5) optical and thermal quenching effects, (6) greater forward current under illumination than in the dark, (7) temperature independence of I - V characteristics, and (8) persistence of enhanced photocurrent for long times. These results can be qualitatively explained by a simple model of the band profile.

In this model, a conduction band spike acts as a gate to photoexcited electrons tunneling from the Cu_2S to the CdS. The width of the spike is controlled by deep impurity levels in the CdS-depletion layer whose occupancy is modulated by light.¹¹

The proposed band profile for nonheat-treated Cu_2S -CdS heterojunctions is shown in Fig. 11(a). The Cu_2S is represented as a degenerate or nearly degenerate p -type semiconductor.^{12,13} The CdS far from the interface is a low resistivity (0.1–1.0 $\Omega \text{ cm}$) n -type semiconductor. At the interface, a conduction band spike results from differences in the electron affinities of the two materials or from the presence of interface states. The long-wavelength photovoltaic response of the junction is due to light absorption in the thin Cu_2S layer.⁶ The photoexcited electrons diffuse to the interface, tunnel through the conduction band spike, and are collected by the diffusion potential.

Short heat treatment of the cells at 250°C causes rapid diffusion of acceptor imperfections (with ground state) at energy level E_2 and hole excited state at E_1 into a narrow layer of CdS.¹⁴ Compensation of the

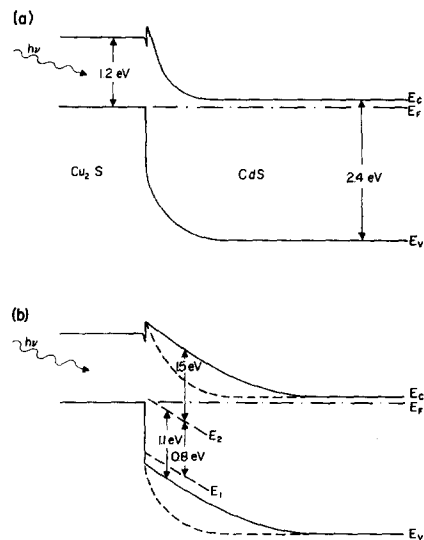


FIG. 11. Band profiles of the Cu_2S -CdS heterojunction (a) before heat treatment and (b) after heat treatment. The solid lines show equilibrium band profile and the dashed lines show the steady-state band profile under illumination such that levels E_2 are filled with holes.

CdS by the charged acceptor states changes the band profile to that shown in Fig. 11(b). The conduction band spike is considerably wider; photoexcited electrons in the Cu_2S can no longer tunnel through, and the long-wavelength response is decreased. The occupancy of these imperfections controls the depletion width in the CdS . Hole trapping decreases the ionized acceptor density resulting in depletion-layer narrowing. The band profile changes as indicated by the dashed lines to a profile approaching the preheat-treatment shape. Narrowing of the depletion region reduces the width of the conduction band spike, increasing its transparency to electrons tunneling from the Cu_2S . Holes may be trapped in level E_2 either by optical excitation of electrons from the imperfection to the conduction band or by band-to-band excitation followed by hole capture.

Holes trapped in levels E_2 can be released optically by the transitions indicated on the diagram. Hole emptying by this process corresponds to optical quenching in two infrared bands, one of which is thermally assisted. Thermal quenching, in which holes are thermally excited to the valence band, or capture of electrons from the conduction band are other possible mechanisms emptying the levels of holes. Emptying of trapped holes increases the ionized acceptor density resulting in widening of the depletion layer and hence decreased transparency of the conduction band spike.

DISCUSSION

All the experimental results on efficient Cu_2S - CdS cells can be understood at least qualitatively in the framework of the proposed model.

The major part of the long-wavelength response in these cells is due to light absorbed in the Cu_2S layer as can be easily established by consideration of the optical absorption of the layer and the observed quantum yields of the junction.

Before heat treatment, the spectral response of the photocurrent is essentially that of the Cu_2S . Since quantum yields of approximately 0.1 are observed, the conduction band spike must be very transparent to tunneling electrons. Assuming a triangular spike 0.1-eV high, the tunneling probability is estimated to be 0.2 for the highly conducting CdS crystals used for these cells.

The temperature dependence of dark forward I - V characteristics suggests that the current is by a tunneling mechanism possibly through interface states. Illumination has no effect on the forward component of current so that forward characteristics under illumination are essentially equal to the dark characteristic minus a constant short-circuit photocurrent.

The changes observed in the properties of the heterojunction after heat treatment can all be explained by assuming that heat treatment has introduced acceptor imperfections in a thin layer of CdS at the junction.

The location of the levels at 0.3 and 1.1 eV above the valence band was determined from the quenching experiments, which had very similar characteristics to quenching of photoconductivity in sensitive CdS crystals. Thermal quenching of the persistence of enhancement (Fig. 10) yielded an activation energy of 0.95 eV for trap E_2 . The difference between the values for this trap depth obtained optically and thermally is similar to that seen in quenching of photoconductivity.¹⁵

In the dark the presence of acceptor impurities widens the depletion layer so that tunneling processes responsible for the forward current are greatly reduced. Illumination of the junction with photons of sufficient energy to excite electrons from levels E_2 to the conduction band (≈ 1.5 eV) decreases the depletion width restoring the forward current to near its preheat-treatment value. This increase in the forward current due to decreasing the depletion width with illumination explains the observed crossover of the dark and illuminated forward I - V characteristics.

The wide depletion layer of heat-treated cells results in low transparency of the conduction band spike to photoexcited electrons from the Cu_2S . For long-wavelength light having $h\nu < 1.5$ eV the photocurrent will be small since light penetrating to the CdS is not sufficiently energetic to change the width of the spike by exciting electrons out of levels E_2 . At photon energies greater than 1.5 eV, light which penetrates to the CdS can cause transitions from levels E_2 to the conduction band. This tends to narrow the depletion layer and increase the tunneling probability for the electrons generated in the Cu_2S . The slow increase of the photocurrent in this spectral region is due to the low optical-absorption coefficient of the impurities in the CdS resulting in a long time to reach steady-state conditions.

When secondary illumination with $h\nu > 1.5$ eV is incident on the junction, the depletion layer is narrowed and the transparency of the spike is increased for electrons generated in the Cu_2S by any wavelength. Thus enhancement of the longest wavelength generated photocurrent is observed.

Optical quenching by secondary light can only be expected when the primary light is sufficiently energetic ($h\nu > 1.5$ eV) to excite electrons from levels E_2 causing enhancement. For enhanced photosignals, transitions at 0.8 and 1.1 eV, which tend to refill the empty levels at E_2 with electrons, result in quenching.

The very long persistence of the effects of secondary illumination, which was demonstrated in Fig. 9 is due to level E_2 being 1.1-eV above the valence band so that thermal emptying of holes at room temperature is extremely slow. Since the traps which control the width of the conduction band spike lie in the depletion region, trap emptying by electron capture from the conduction band is very unlikely because of the low density of free electrons in this region. The long trapping time of holes in levels E_2 also explains the low intensity of

secondary light necessary to saturate the enhancement of the short-circuit photocurrent.

In the model proposed by Shiozawa *et al.*⁶ the resistance of a photoconducting *p*-type CdS layer controls the photocurrent. This resistance would be expected to show up as a greatly increased series resistance in the high forward current region of the dark *I*-*V* characteristics, an effect which is not observed. The long persistence of photocurrent enhancement effects by secondary light is also inconsistent with the photoconductivity explanation. The high density of free carriers in such a layer would be expected to decay rapidly in the dark, at least in the initial dark interval. These facts lead us to conclude that changes in trap occupancy in the compensated CdS region cause changes in the CdS depletion width and hence in the electric field at the interface. This field is the important parameter governing the emission of electrons into the CdS. Changing the electric field at the interface could increase the tunneling transparency of a conduction band spike or possibly could alter the relative amounts of photocurrent to interface recombination current. In either case the photocurrent is controlled by a physical process (tunneling or interface recombination) occurring at the interface.

Although most of the photovoltaic cells studied were made on single crystals of CdS, similar measurements were made on a thin-film heterojunction formed by a dipping technique on evaporated polycrystalline CdS. This cell was found to have qualitatively identical properties to the heat-treated single-crystal cells except that the optical quenching band at 1.55 μm was not observed. The model proposed in this paper is therefore believed to be applicable also to the evaporated CdS cells.

CONCLUSIONS

Experiments before and after heat treatment of carefully prepared Cu₂S-CdS heterojunctions show that well-behaved efficient photovoltaic cells can be made with no heat treatment. These cells have normal light and dark *I*-*V* characteristics and show no effects of secondary light on their photovoltaic characteristics. Heat treatment of the same cells results in slightly increased V_{oc} , probably due to decreased forward current, and decreased I_{sc} , resulting in a net decrease in cell efficiency.

After heat treatment a crossover of the dark and

light *I*-*V* characteristics is observed. Slow transients on the photovoltaic response are seen, and secondary illumination causes quenching and enhancement of the photocurrent.

All the observations can be explained by a model in which a conduction band spike exists at the Cu₂S-CdS interface. The width of the spike, and therefore its transparency to tunneling electrons, is modified by trapping of holes in deep-lying imperfection levels introduced into a narrow layer of CdS by the heat treatment.

* Sponsored by the National Aeronautics and Space Administration through Lewis Research Center, Cleveland, Ohio.

† Present address: IBM Corporation, Research Division, San Jose, Calif. 95100.

¹ D. A. Cusano, IRE Trans. Electron Devices **9**, 504 (1962).

² B. Selle, W. Ludwig, and R. Mach, Phys. Status Solidi **24**, K149 (1967).

³ P. N. Keating, J. Phys. Chem. Solids **24**, 1101 (1963); J. Appl. Phys. **36**, 564 (1965).

⁴ N. Duc Cuong and J. Blair, J. Appl. Phys. **37**, 1660 (1966).

⁵ R. J. Mytton, Brit. J. Appl. Phys. **1**, 721 (1968).

⁶ L. R. Shiozawa, G. A. Sullivan, and F. Augustine, Proc. Photovoltaic Specialists Conf. 7th, Pasadena, Calif., 30, 1968; L. R. Shiozawa, F. Augustine, G. A. Sullivan, J. M. Smith III, and W. R. Cook, Jr., "Research on the Mechanism of the Photovoltaic Effect in High Efficiency CdS Thin-Film Solar Cells," Clevite Corp. Rept, contract AF 33(615)-5224, 1969.

⁷ A. E. Potter, Jr., W. B. Berry, H. W. Brandhorst, Jr., and R. L. Schalla, NASA Tech. Note, NASA TN D-4333 (1968).

⁸ A. E. Potter, Jr., R. L. Schalla, H. W. Brandhorst, Jr., and L. Rosenblum, NASA Tech. Mem., NASA TM X-52500 (1968).

⁹ A. E. van Aershot, J. J. Capart, K. H. David, M. Fabricotti, K. H. Heffels, J. J. Loferski, and K. K. Reinhardt, Ref. 6, p. 30.

¹⁰ W. D. Gill and R. H. Bube, J. Appl. Phys. **41**, 1694 (1970).

¹¹ A possible alternative to the conduction band spike is a model in which recombination through interface states competes with carrier collection by the diffusion potential. Modulation of the CdS depletion width by light would change the field at the interface altering the ratio of photocurrent to interface recombination current.

¹² E. Hirahara, J. Phys. Soc. Japan **6**, 428 (1951).

¹³ G. B. Abdulleav, Z. A. Aliyova, E. H. Zamanova, and G. A. Asadov, Phys. Status Solidi **26**, 65 (1968).

¹⁴ Because of the similarity of optical and thermal quenching data to quenching of photoconductivity [R. H. Bube, Phys. Rev. **99**, 1105 (1955); and S. O. Hemila and R. H. Bube, J. Appl. Phys. **38**, 5258 (1967)] and excitation of ir emission [F. J. Bryant and A. F. J. Cox, Brit. J. Appl. Phys. **16**, 463 (1965); and Proc. Phys. Soc. (London) **87**, 551 (1966)] in CdS, the imperfection level structure is assumed to be the same. Recent results by P. F. Lindquist and R. H. Bube (private communication) on optical and thermal quenching of photocapacitance in Cu₂S-CdS heterojunctions show a different temperature dependence for the optical quenching of photocapacitance by the long-wavelength band than is found for quenching of photoconductivity. This suggests that the long-wavelength transitions observed here may not be the same as those found in photoconductivity of CdS.

¹⁵ R. H. Bube, J. Appl. Phys. **35**, 586 (1964).